



# The coronal parameters of local Seyfert galaxies

Andrea Marinucci  
(Roma Tre)

on behalf of the  
NuSTAR AGN Physics WG

From the Dolomites to the event horizon:  
Sledging down to the Black Hole Potential Well (3<sup>rd</sup> edition)  
Sesto Val Pusteria  
July 13, 2015

# Overview

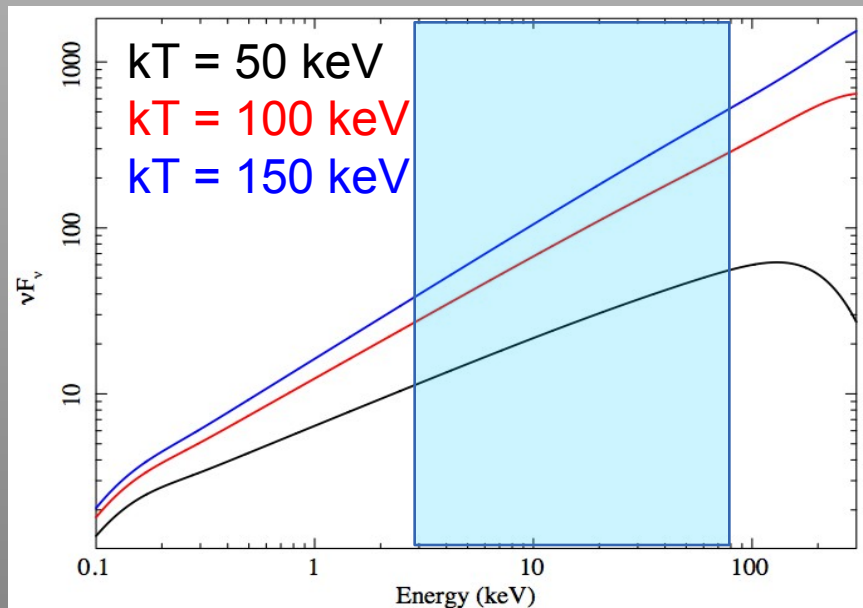
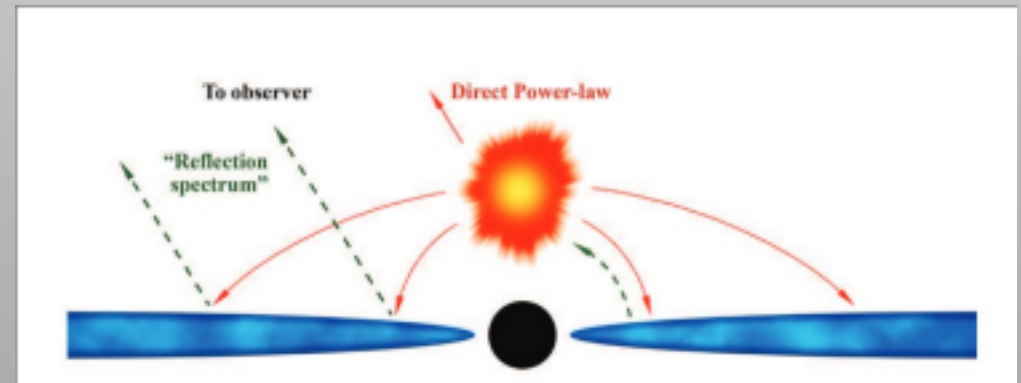
- Brief introduction on high-energy cutoff measurements
  - Nearby AGN seen by NuSTAR
    - Results
- Conclusions and future perspectives

- Brief introduction on high-energy cutoff measurements
  - Nearby AGN seen by NuSTAR
    - Results
  - Conclusions and future perspectives

# Introduction

One of the main open problem for AGN is the nature of the primary X-ray emission.

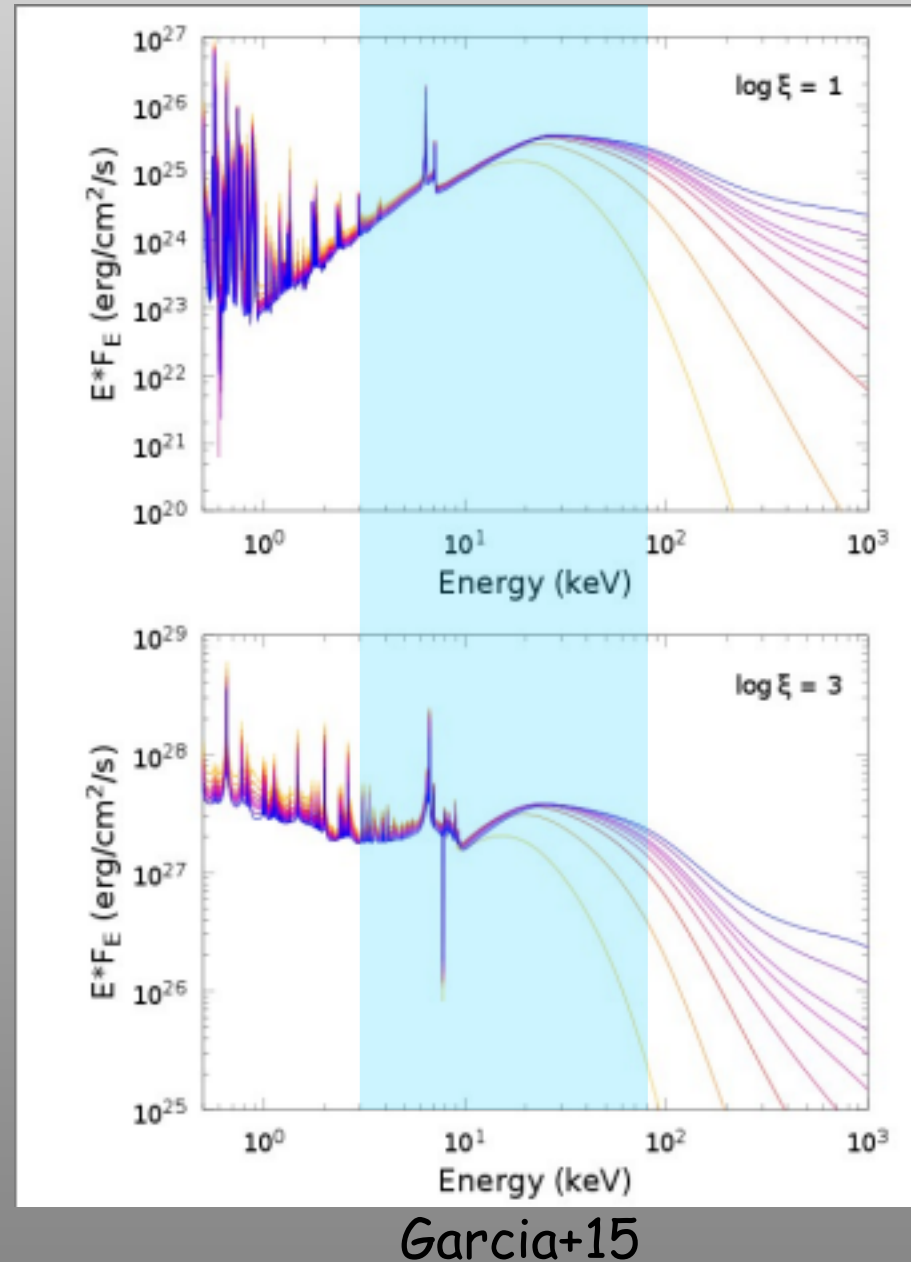
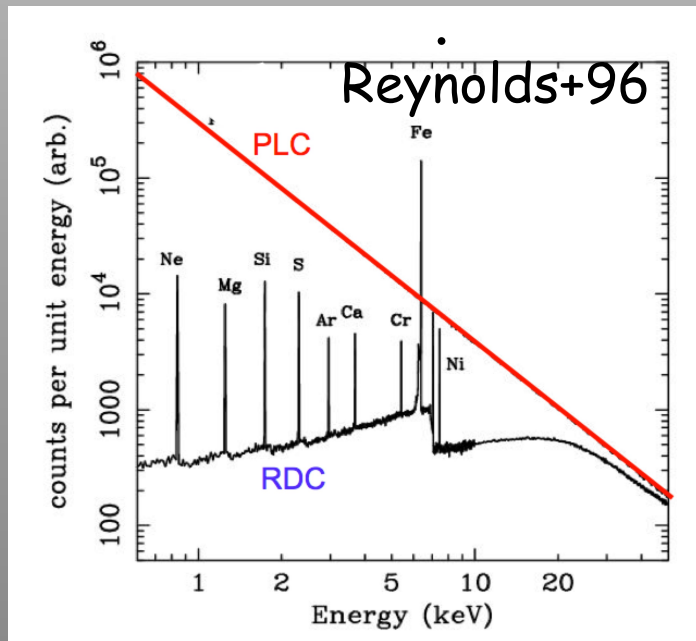
It is due to Comptonization of soft photons, but the geometry, optical depth and temperature of the emitting corona are largely unknown.



Most popular models imply  $E_{\text{cut}} = 2-3 \times kT_e$ , so measuring  $E_{\text{cut}}$  helps constraining Comptonization models.

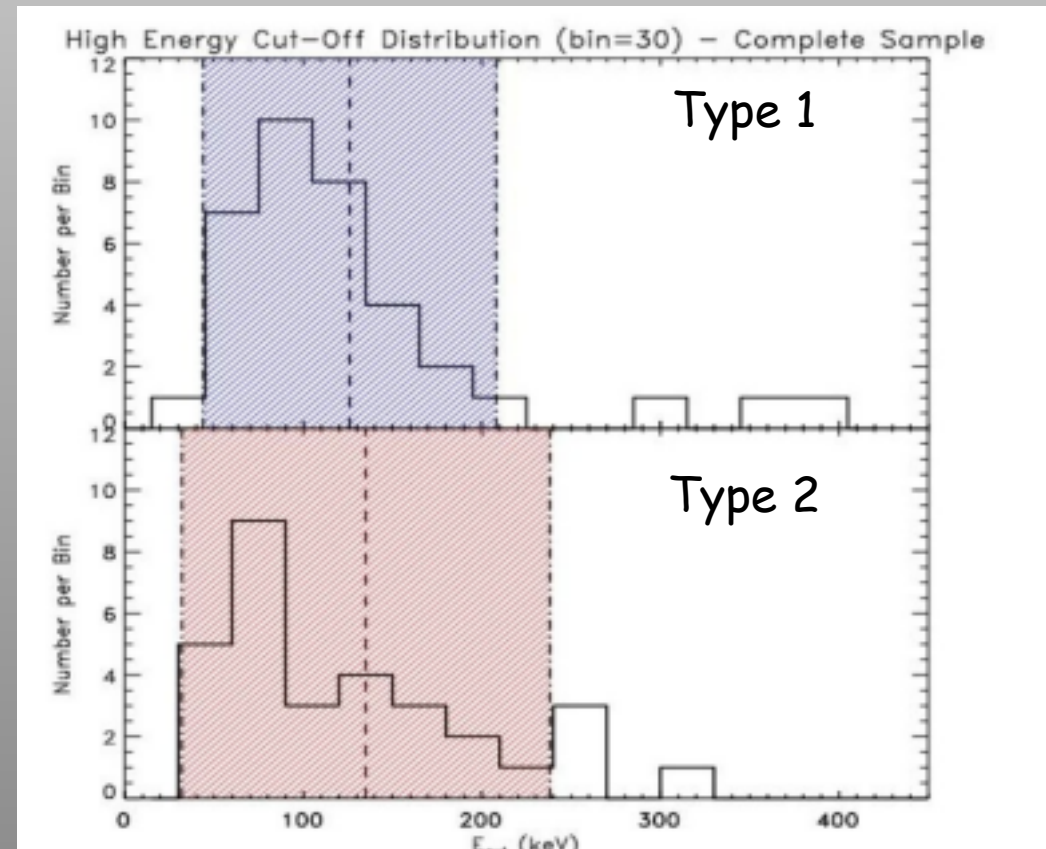
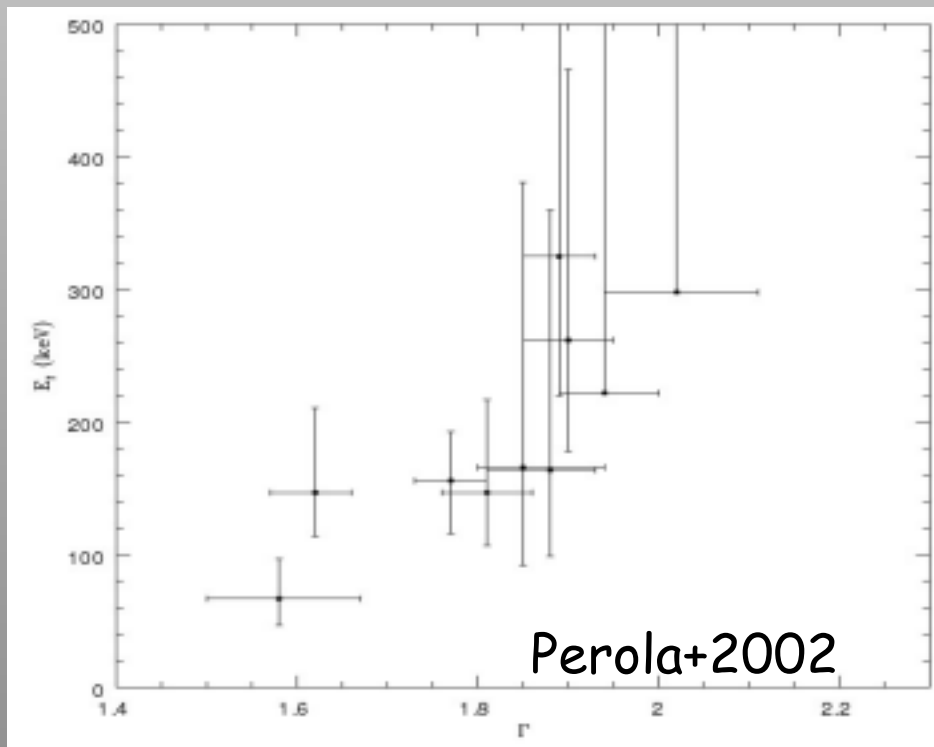
# Introduction

Since the primary X-ray radiation illuminates the disc and is partly reflected towards the observer's line of sight it is fundamental to properly take it into account: Xillver (Garcia+13), KYreflionx (see Michal's and Jiri's talks).



# Introduction

So far, we have only a handful of results based on non focusing, and therefore strongly background-dominated, satellites (BeppoSAX-PDS, Suzaku HXD-PIN, INTEGRAL, Swift-BAT)



De Rosa+2012; Molina+2013

- Brief introduction on high-energy cutoff measurements
  - Nearby AGN seen by NuSTAR
    - Results
- Conclusions and future perspectives

# The NuSTAR satellite

## Nuclear Spectroscopic Telescope Array

### 1 Ms Sensitivity

$3.2 \times 10^{-15}$  erg/cm<sup>2</sup>/s ( 6 – 10 keV)

$1.4 \times 10^{-14}$  erg/cm<sup>2</sup>/s (10 – 30 keV)

### Imaging

HPD 58"

FWHM 18"

Localization 2" (1-sigma)

Harrison+13

### Spectral response

energy range: 3-79 keV

$\Delta E$  @ 6 keV 0.4 keV FWHM

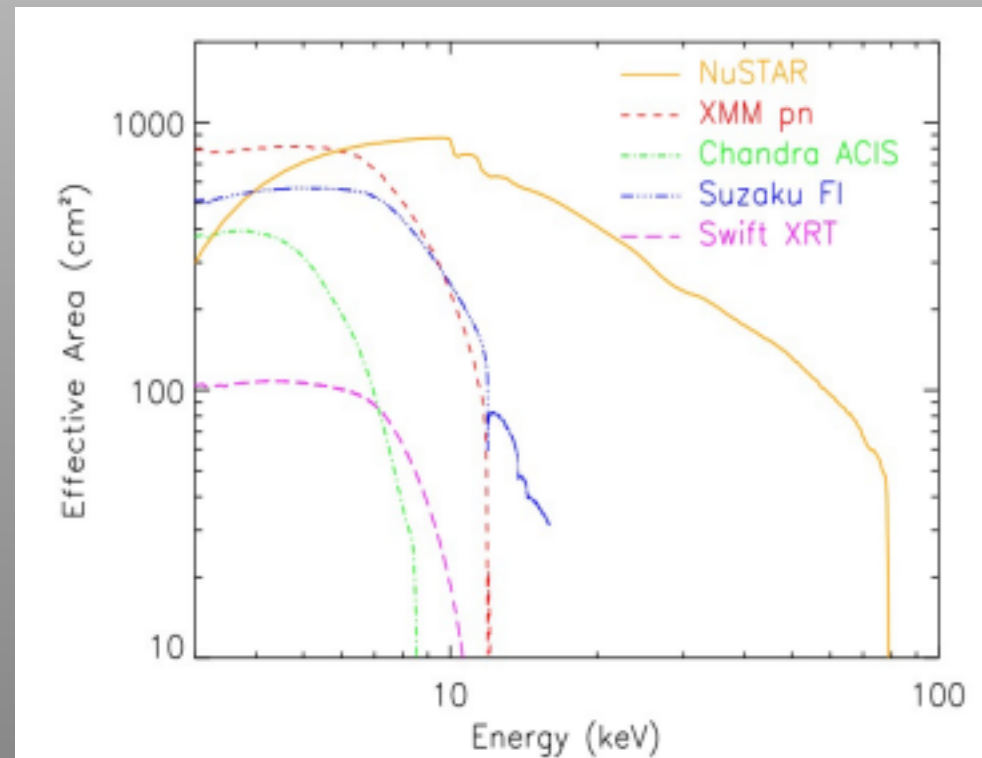
$\Delta E$  @ 60 keV 1.0 keV FWHM

### Target of Opportunity

response <24 hr

typical 6-8 hours

80% sky accessibility

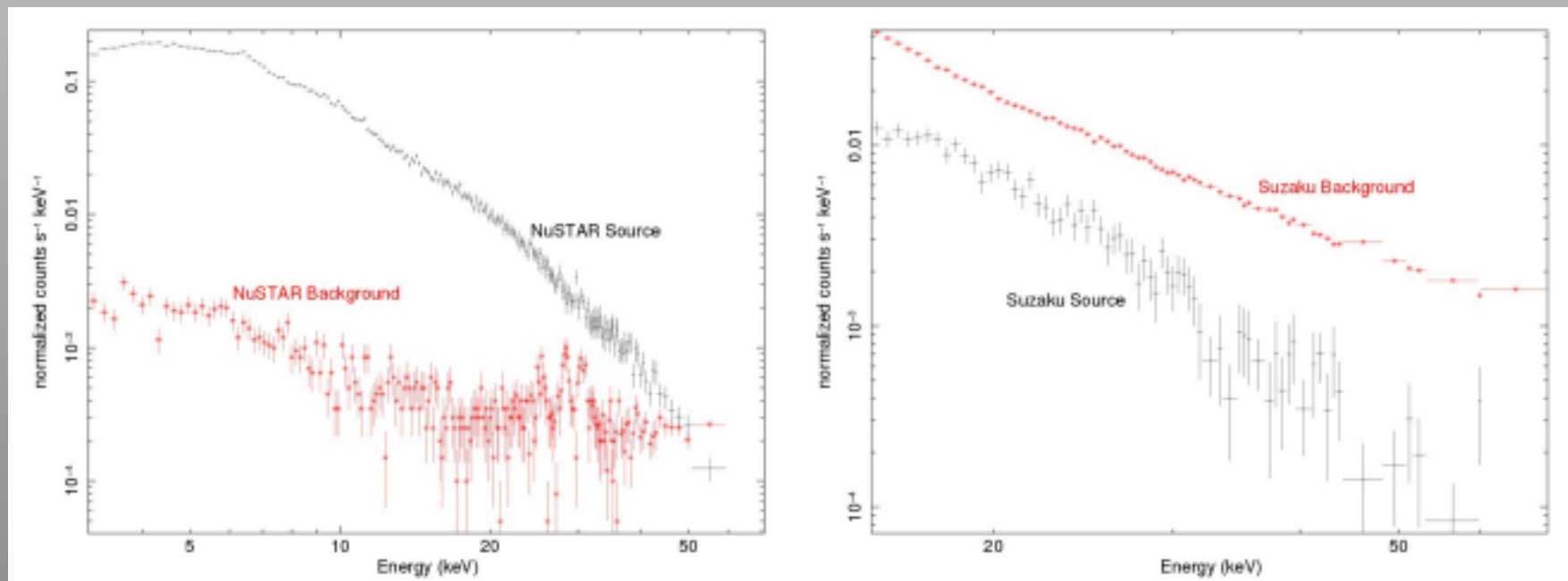




# The NuSTAR satellite

The combination of NuSTAR high effective area and low background yields  
~100x better S/N versus Suzaku HXD-PIN

MCG-6-30-15: 125 ks net exposure time and same 15-70 keV flux ( $6.5 \times 10^{-11}$   
 $\text{erg}/\text{cm}^2/\text{s}$ )



Marinucci+14

# Nearby AGN seen by NuSTAR

Source	$z$	$\log(M)$ [ $M_{\odot}$ ]	$r_{\text{co}}$ [ $r_G$ ]	$F_x$	$E_{\text{cut}}$ [keV]	$\Gamma$	$\Theta$	$\ell$	Data	References
NGC 5506	0.006	$8 \pm 1$	10	2.9	$720^{+130}_{-190}$	$1.91^{+0.03}_{-0.03}$	$0.71^{+0.13}_{-0.36}$	$4^{+33}_{-3}$	SWIFT/NU	1–2
NGC7213	0.006	$7.98^{+0.22}_{-0.24}$	10	0.71	> 240	$1.84^{+0.03}_{-0.03}$	> 0.05	$1.0^{+0.7}_{-0.4}$	NU	3–4
MCG-6-30-15	0.008	$6.7 \pm 1$	2.9	8.2	> 110	$2.061^{+0.005}_{-0.005}$	> 0.04	$258^{+2323}_{-232}$	XMM/NU	5–6
NGC 2110	0.008	$8.3 \pm 1$	10	8.9	> 210	$1.64^{+0.03}_{-0.03}$	> 0.07	$10^{+89}_{-9}$	SWIFT/NU	7–8
MCG 5-23-16	0.009	$7.85 \pm 1$	10	4.2	$116^{+6}_{-5}$	$1.85^{+0.01}_{-0.01}$	$0.11^{+0.01}_{-0.04}$	$15^{+136}_{-14}$	NU	9–11
SWIFT J2127.4+5654	0.014	$7.18 \pm 1$	13	1.1	$108^{+11}_{-10}$	$2.08^{+0.01}_{-0.01}$	$0.11^{+0.01}_{-0.04}$	$34^{+308}_{-31}$	XMM/NU	12–13
IC4329A	0.016	$8.1 \pm 1$	10	4.9	$186^{+14}_{-14}$	$1.73^{+0.01}_{-0.01}$	$0.18^{+0.01}_{-0.07}$	$41^{+365}_{-37}$	SU/NU	14–15
NGC 5548	0.018	$7.59^{+0.24}_{-0.21}$	4.5	1.3	$70^{+40}_{-10}$	$1.49^{+0.05}_{-0.05}$	$0.07^{+0.04}_{-0.03}$	$88^{+55}_{-37}$	XMM/NU	5, 16–17
Mrk 335	0.026	$7.42^{+0.12}_{-0.16}$	3	0.10	> 174	$2.14^{+0.02}_{-0.04}$	> 0.06	$36^{+16}_{-9}$	SWIFT/NU	18–19
Ark 120	0.033	$7.66^{+0.05}_{-0.06}$	4.4	0.55	> 68	$1.73^{+0.02}_{-0.02}$	> 0.06	$4^{+1}_{-1}$	XMM/NU	20–21
1H0707-495	0.041	$6.31 \pm 1$	2	0.14	> 63	$3.2^{+0.2}_{-0.2}$	> 0.02	$358^{+3219}_{-322}$	SWIFT/NU	22–23
Fairall 9	0.047	$8.41^{+0.11}_{-0.09}$	21	0.87	> 242	$1.96^{+0.01}_{-0.02}$	> 0.08	$12^{+3}_{-3}$	XMM/NU	20, 24
3C390.3	0.056	$9.40^{+0.05}_{-0.06}$	10	1.6	$116^{+24}_{-8}$	$1.70^{+0.01}_{-0.01}$	$0.11^{+0.02}_{-0.04}$	$18^{+3}_{-2}$	SU/NU	25–26
Cyg A	0.056	$9.40^{+0.11}_{-0.14}$	10	1.1	> 110	$1.47^{+0.13}_{-0.06}$	> 0.04	$6^{+2}_{-1}$	NU	27–28
3C382	0.058	$9.2 \pm 0.5$	10	1.4	$214^{+147}_{-63}$	$1.68^{+0.03}_{-0.02}$	$0.21^{+0.14}_{-0.11}$	$12^{+25}_{-8}$	SWIFT/NU	29–30

$F_x$  is the 0.1-200 keV X-ray flux in  $10^{-10} \text{ erg cm}^{-2} \text{ s}^{-1}$ .

**References:** 1: Guainazzi et al. (2010), 2: Matt et al. (2015), 3: Ursini et al. (2015b), 4: Blank, Harnett & Jones (2005), 5: Emmanoulopoulos et al. (2014), 6: Marinucci et al. (2014c), 7: Moran et al. (2007), 8: Marinucci et al. (2014a), 9: Ponti et al. (2012), 10: Zoghbi et al. (2014), 11: Baloković et al. (2015), 12: Malizia et al. (2008), 13: Marinucci et al. (2014b), 14: Bianchi et al. (2009), 15: Brenneman et al. (2014), 16: Pancoast et al. (2014), 17: Ursini et al. (2015a), 18: Grier et al. (2012), 19: Parker et al. (2014), 20: Peterson et al. (2004), 21: Matt et al. (2014), 22: Bian & Zhao (2003), 23: Kara et al. (2015), 24: Lohfink & Reynolds (2015), 25: Grier et al. (2013), 26: Lohfink & Tombesi (2015), 27: Tadhunter et al. (2003), 28: Reynolds et al. (2015), 29: Winter et al. (2009), 30: Ballantyne et al. (2014)

Fabian+15

# Nearby AGN seen by NuSTAR

Source	$z$	$\log(M)$ [ $M_{\odot}$ ]	$r_{\text{co}}$ [ $r_G$ ]	$F_x$	$E_{\text{cut}}$ [keV]	$\Gamma$	$\Theta$	$\ell$	Data	References
NGC 5506	0.006	$8 \pm 1$	10	2.9	$720^{+130}_{-190}$	$1.91^{+0.03}_{-0.03}$	$0.71^{+0.13}_{-0.36}$	$4^{+33}_{-3}$	SWIFT/NU	1–2
NGC7213	0.006	$7.98^{+0.22}_{-0.24}$	10	0.71	$> 240$	$1.84^{+0.03}_{-0.03}$	$> 0.05$	$1.0^{+0.7}_{-0.4}$	NU	3–4
MCG-6-30-15	0.008	$6.7 \pm 1$	2.9	8.2	$> 110$	$2.061^{+0.005}_{-0.005}$	$> 0.04$	$258^{+2323}_{-232}$	XMM/NU	5–6
NGC 2110	0.008	$8.3 \pm 1$	10	8.9	$> 210$	$1.64^{+0.03}_{-0.03}$	$> 0.07$	$10^{+89}_{-9}$	SWIFT/NU	7–8
MCG 5-23-16	0.009	$7.85 \pm 1$	10	4.2	$116^{+6}_{-5}$	$1.85^{+0.01}_{-0.01}$	$0.11^{+0.01}_{-0.04}$	$15^{+136}_{-14}$	NU	9–11
SWIFT J2127.4+5654	0.014	$7.18 \pm 1$	13	1.1	$108^{+11}_{-10}$	$2.08^{+0.01}_{-0.01}$	$0.11^{+0.01}_{-0.04}$	$34^{+308}_{-31}$	XMM/NU	12–13
IC4329A	0.016	$8.1 \pm 1$	10	4.9	$186^{+14}_{-14}$	$1.73^{+0.01}_{-0.01}$	$0.18^{+0.01}_{-0.07}$	$41^{+365}_{-37}$	SU/NU	14–15
NGC 5548	0.018	$7.59^{+0.24}_{-0.21}$	4.5	1.3	$70^{+40}_{-10}$	$1.49^{+0.05}_{-0.05}$	$0.07^{+0.04}_{-0.03}$	$88^{+55}_{-37}$	XMM/NU	5, 16–17
Mrk 335	0.026	$7.42^{+0.12}_{-0.16}$	3	0.10	$> 174$	$2.14^{+0.02}_{-0.04}$	$> 0.06$	$36^{+16}_{-9}$	SWIFT/NU	18–19
Ark 120	0.033	$7.66^{+0.05}_{-0.06}$	4.4	0.55	$> 68$	$1.73^{+0.02}_{-0.02}$	$> 0.06$	$4^{+1}_{-1}$	XMM/NU	20–21
IH0707-495	0.041	$6.31 \pm 1$	2	0.14	$> 63$	$3.2^{+0.2}_{-0.2}$	$> 0.02$	$358^{+3219}_{-322}$	SWIFT/NU	22–23
Fairall 9	0.047	$8.41^{+0.11}_{-0.09}$	21	0.87	$> 242$	$1.96^{+0.01}_{-0.02}$	$> 0.08$	$12^{+3}_{-3}$	XMM/NU	20, 24
3C390.3	0.056	$9.40^{+0.05}_{-0.06}$	10	1.6	$116^{+24}_{-8}$	$1.70^{+0.01}_{-0.01}$	$0.11^{+0.02}_{-0.04}$	$18^{+3}_{-2}$	SU/NU	25–26
Cyg A	0.056	$9.40^{+0.11}_{-0.14}$	10	1.1	$> 110$	$1.47^{+0.13}_{-0.06}$	$> 0.04$	$6^{+2}_{-1}$	NU	27–28
3C382	0.058	$9.2 \pm 0.5$	10	1.4	$214^{+147}_{-63}$	$1.68^{+0.03}_{-0.02}$	$0.21^{+0.14}_{-0.11}$	$12^{+25}_{-8}$	SWIFT/NU	29–30

$F_x$  is the 0.1-200 keV X-ray flux in  $10^{-10} \text{ erg cm}^{-2} \text{ s}^{-1}$ .

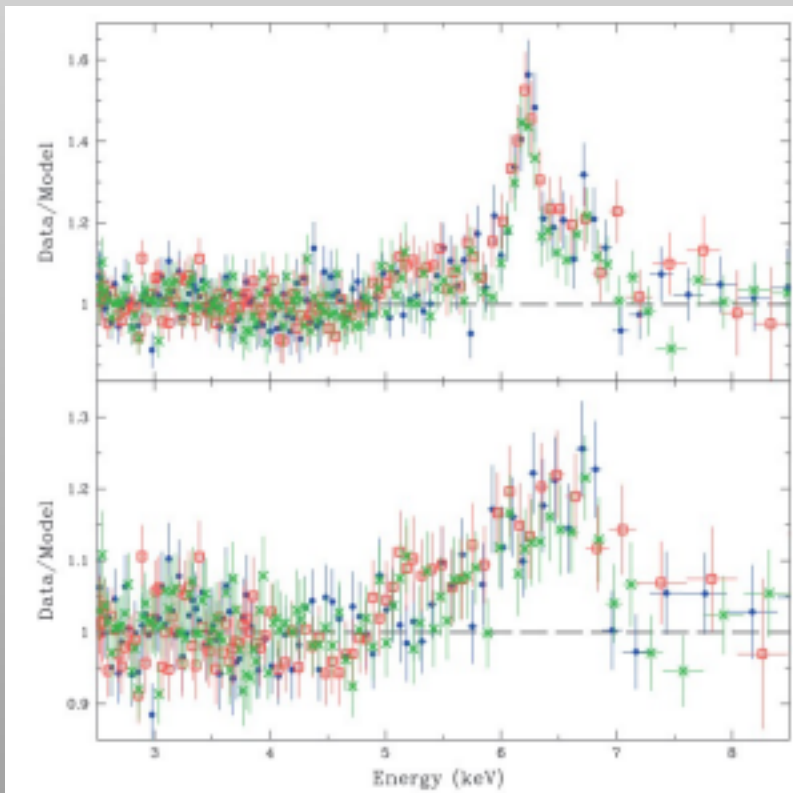
**References:** 1: Guainazzi et al. (2010), 2: Matt et al. (2015), 3: Ursini et al. (2015b), 4: Blank, Harnett & Jones (2005), 5: Emmanoulopoulos et al. (2014), 6: Marinucci et al. (2014c), 7: Moran et al. (2007), 8: Marinucci et al. (2014a), 9: Ponti et al. (2012), 10: Zoghbi et al. (2014), 11: Baloković et al. (2015), 12: Malizia et al. (2008), 13: Marinucci et al. (2014b), 14: Bianchi et al. (2009), 15: Brenneman et al. (2014), 16: Pancoast et al. (2014), 17: Ursini et al. (2015a), 18: Grier et al. (2012), 19: Parker et al. (2014), 20: Peterson et al. (2004), 21: Matt et al. (2014), 22: Bian & Zhao (2003), 23: Kara et al. (2015), 24: Lohfink & Reynolds (2015), 25: Grier et al. (2013), 26: Lohfink & Tombesi (2015), 27: Tadhunter et al. (2003), 28: Reynolds et al. (2015), 29: Winter et al. (2009), 30: Ballantyne et al. (2014)

Fabian+15

- Brief introduction on high-energy cutoff measurements
  - Nearby AGN seen by NuSTAR
    - **Results**
  - Conclusions and future perspectives



# Ark 120

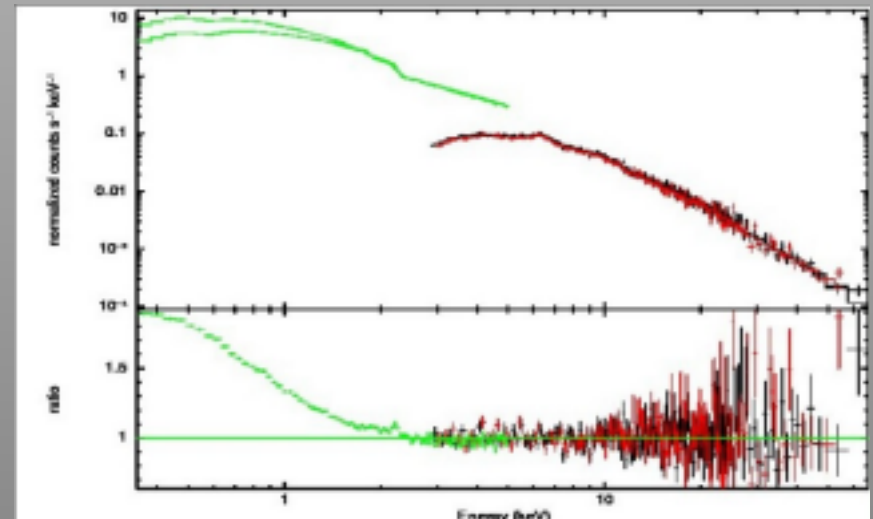


Nardini+11

- Observed simultaneously by  
NuSTAR and XMM for 90 ks in  
2013

(and then again in 2014, see  
Delphine's talk )

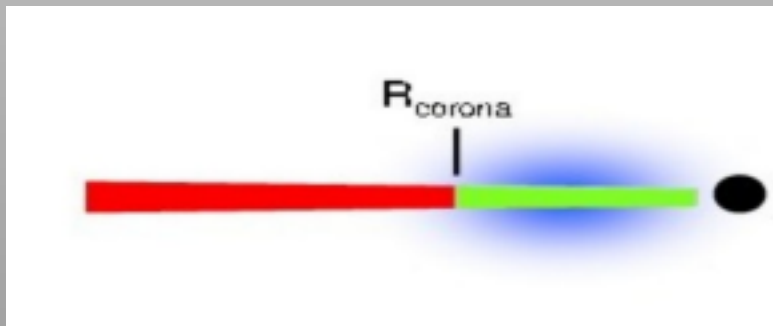
- "Bare" Seyfert 1 galaxy,  
 $F_{2-10 \text{ keV}} \sim 2-4 \times 10^{-11} \text{ erg/cm}^2/\text{s}$
- Relativistic Iron line  
(Suzaku, Nardini+11)
- Prominent soft excess  
(XMM, Vaughan+04)



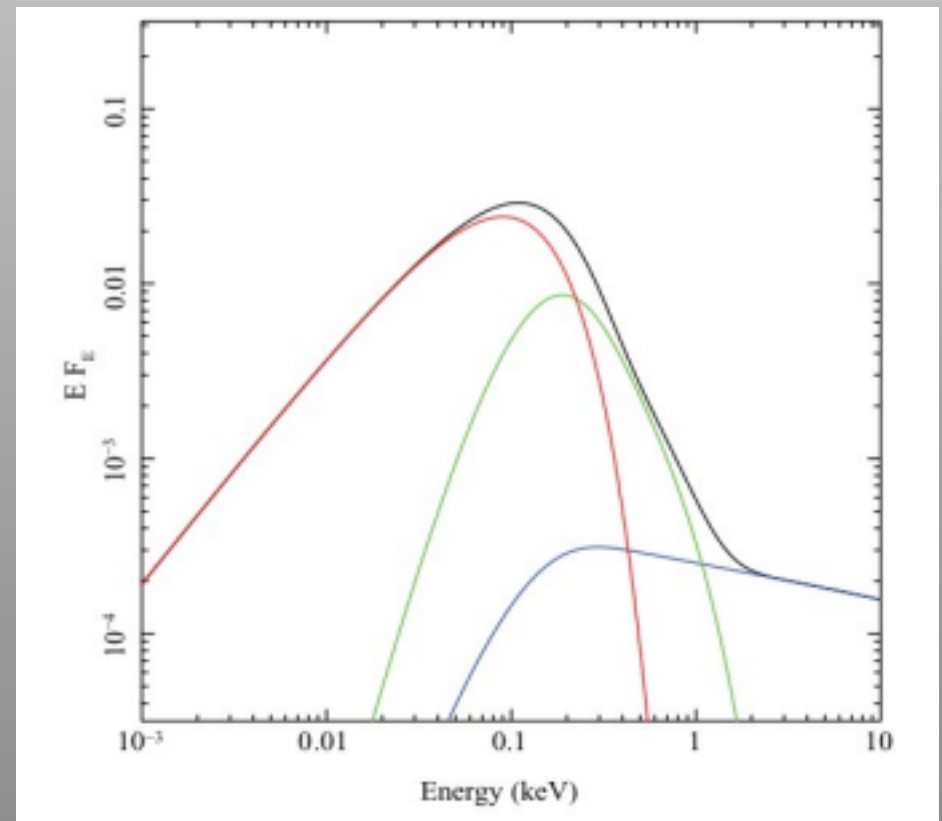
Matt+2014

# Ark 120

The broad-band best fit is with a Comptonization model for the soft excess. Optxagnf (Done+2012) is a disk/corona emission model which assumes a thermal disk emission outside the coronal radius, and soft and hard Comptonization inside.



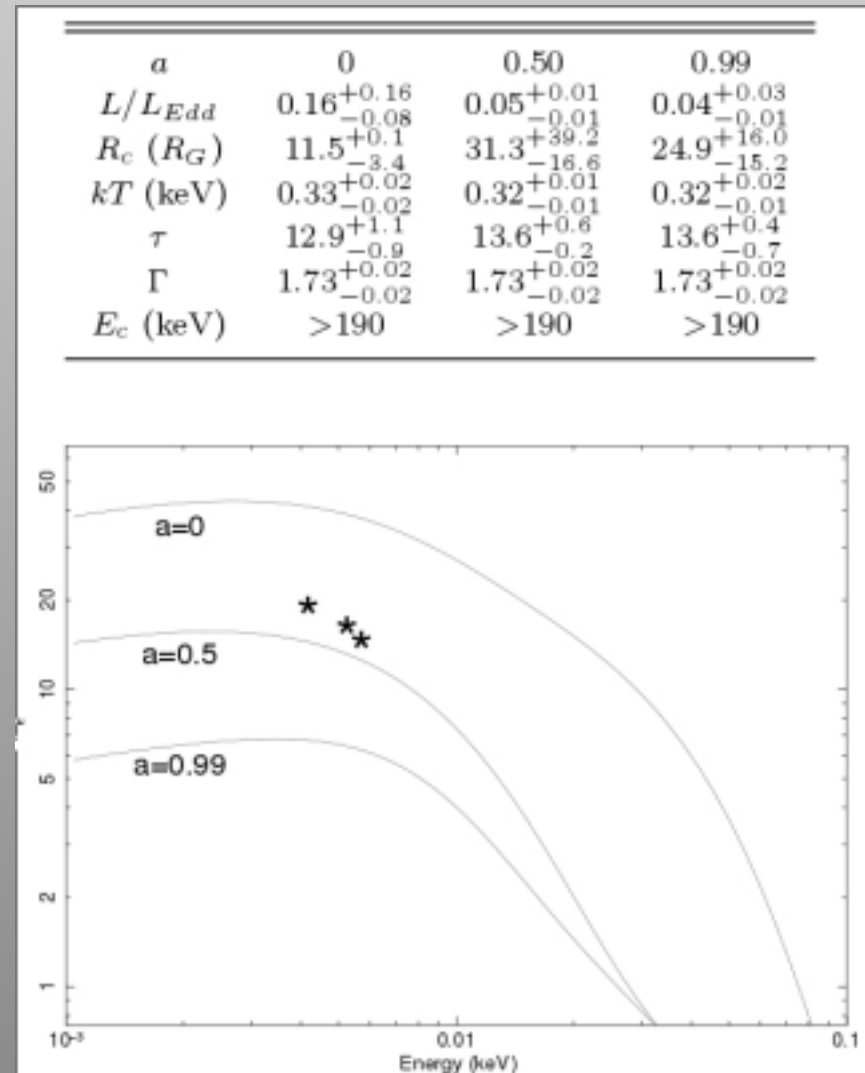
Done+12



# Ark 120

Matt+2014

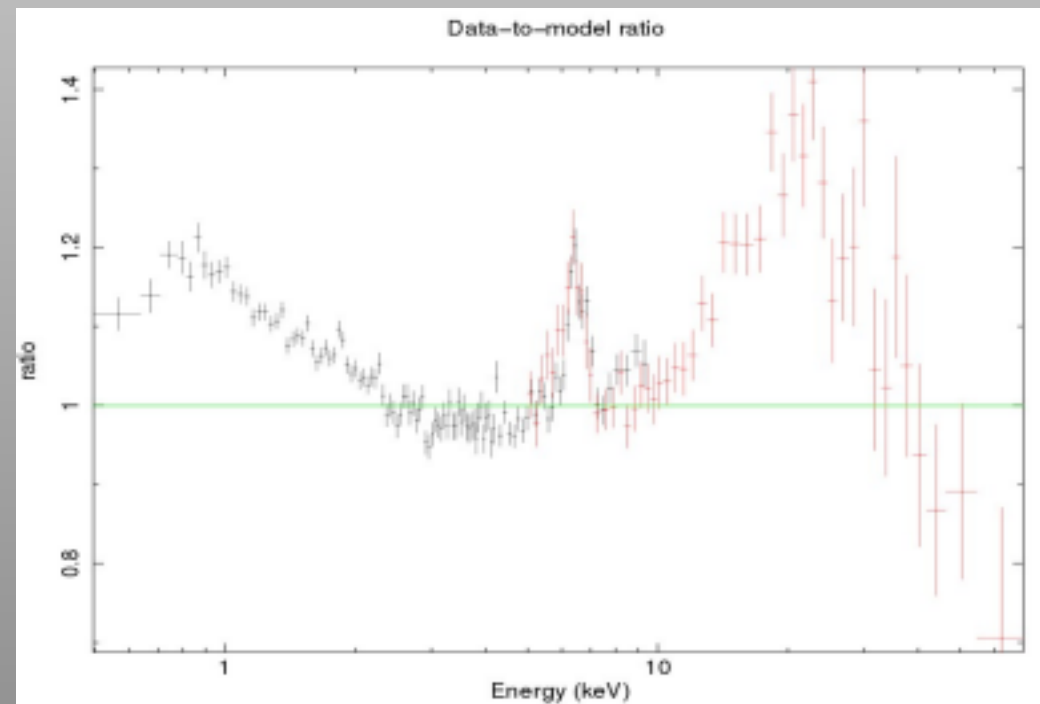
Fluxes from the Optical Monitor  
on board on XMM-Newton  
support an intermediate value for  
the black hole spin.



# Swift J2127.4+5654

NLS1 with a relativistically broadened Fe K $\alpha$  emission line ( $a=0.6\pm 0.2$ ), a steep continuum ( $\Gamma=2-2.4$ ),  $E_c=30-90$  keV,  $L_{\text{bol}}/L_{\text{Edd}}\sim 0.18$  (Miniutti+09, Malizia+08, Panessa+11, Sanfrutos+13)

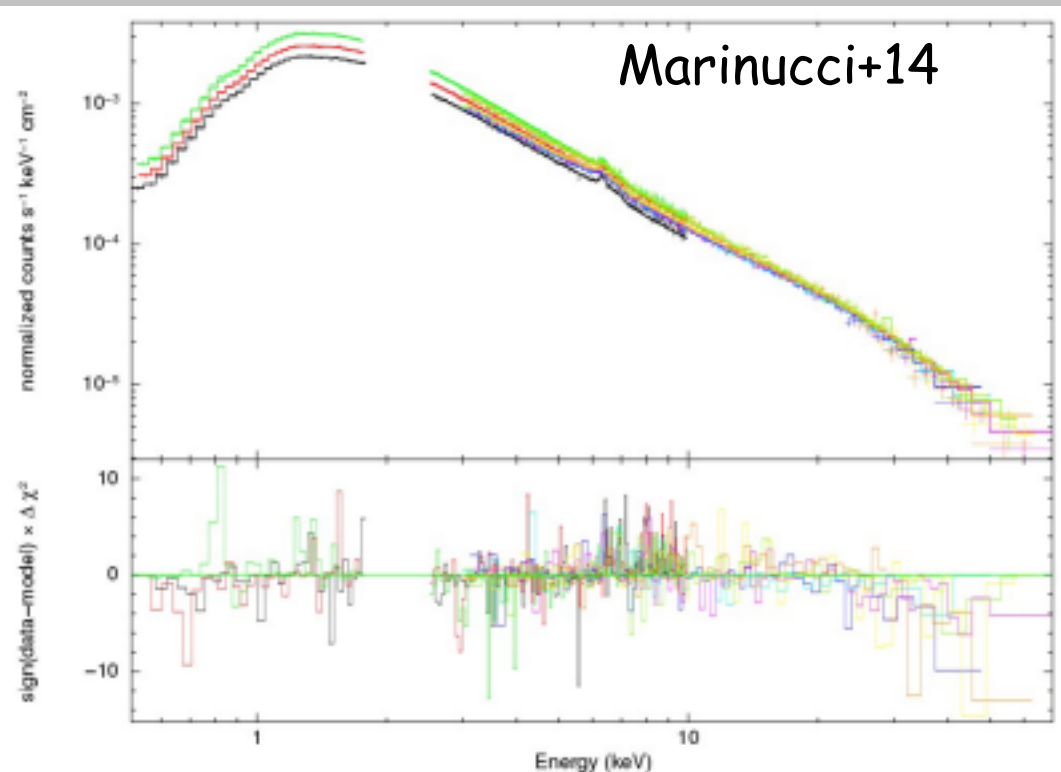
It was observed simultaneously with XMM-Newton for  $\sim 300$  ks and both a strong Compton Hump and a broad Fe K $\alpha$  line are present





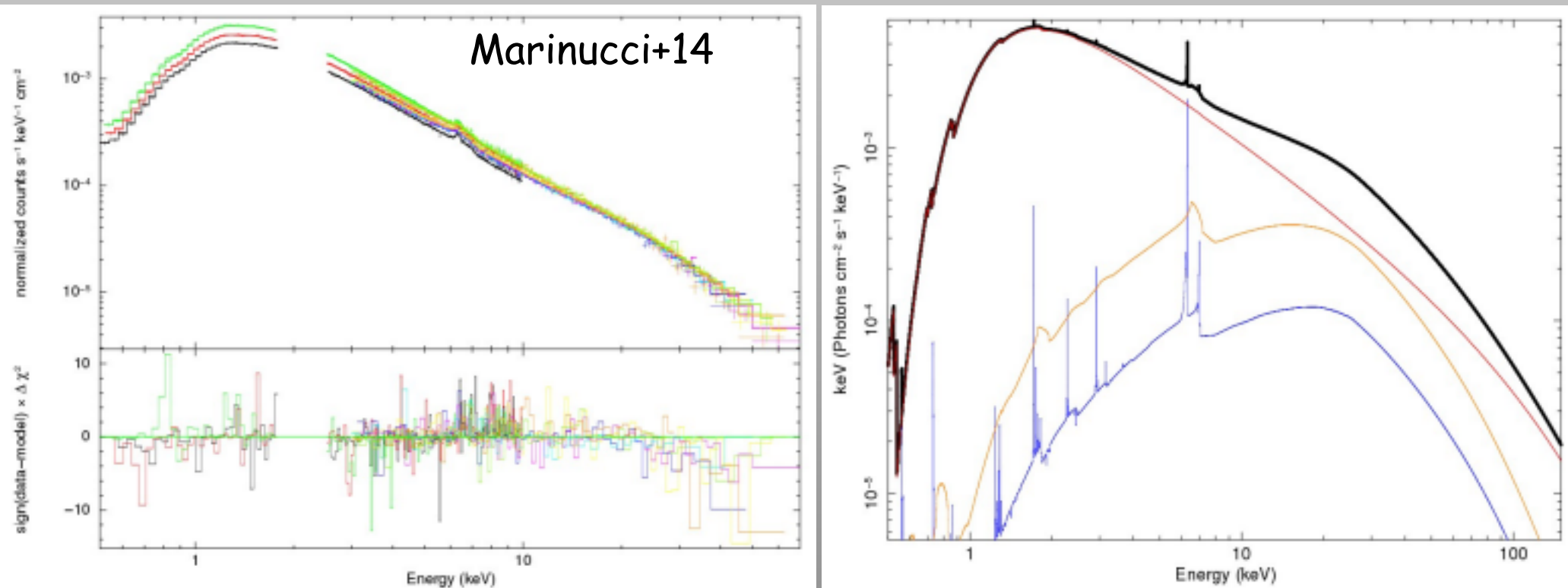
# Swift J2127.4+5654

When a model composed of a primary continuum, relativistic and distant reflection components is applied to the data the only residuals are above  $\sim 25$  keV



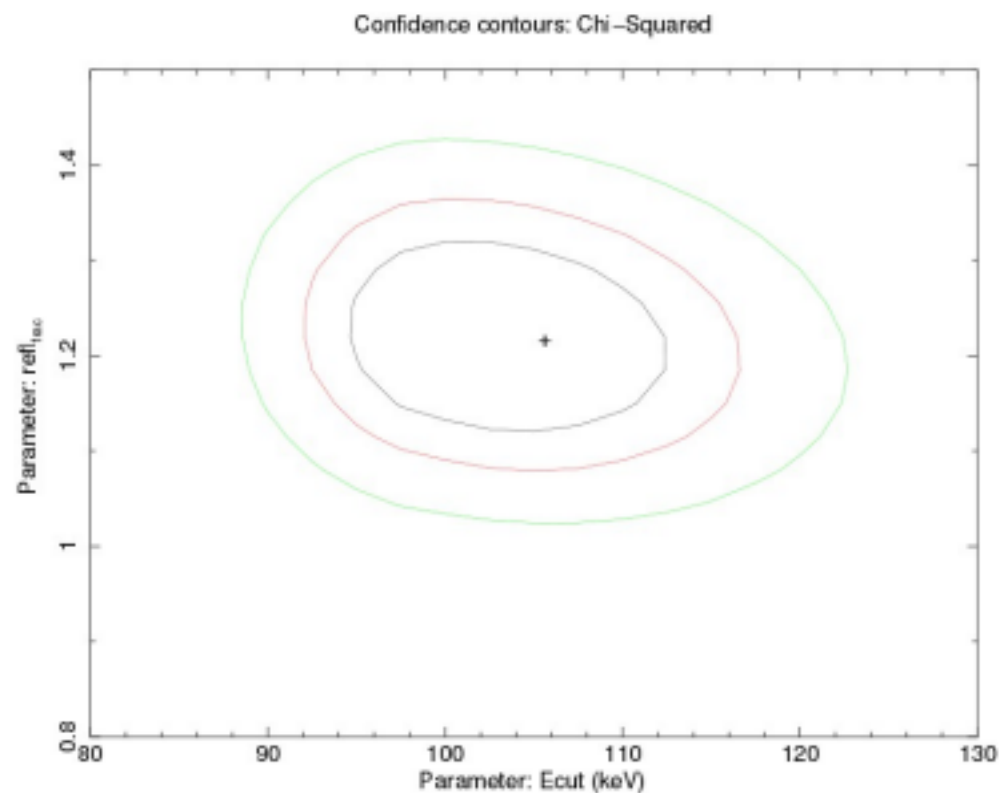
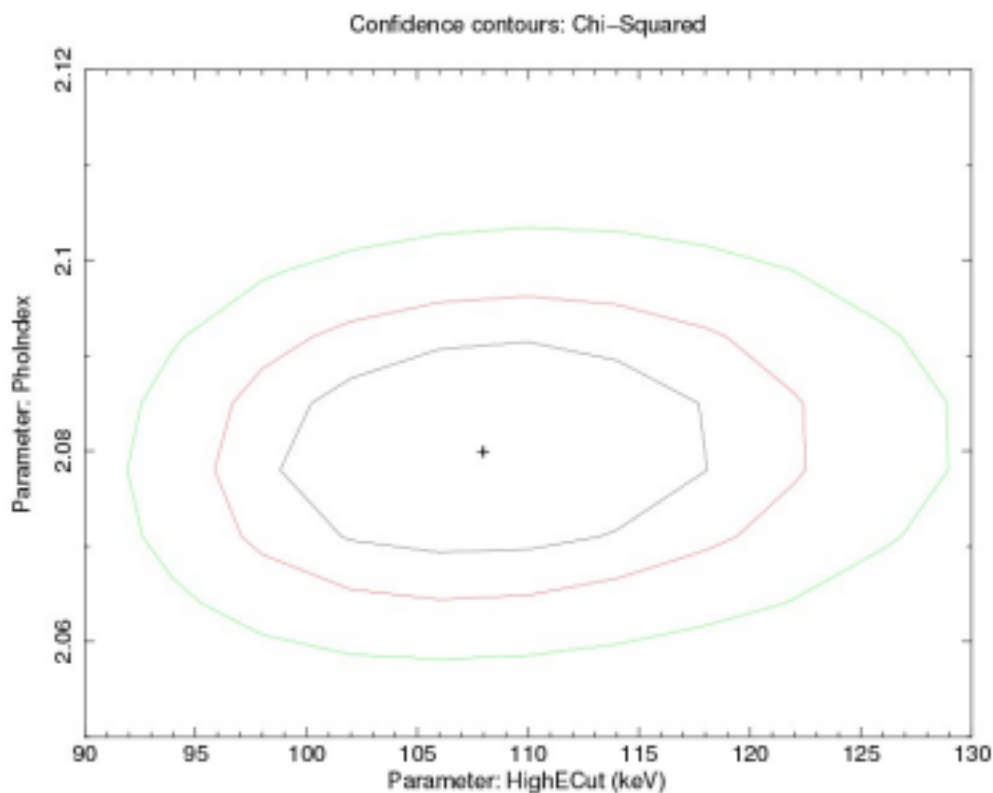
# Swift J2127.4+5654

When a model composed of a primary continuum, relativistic and distant reflection components is applied to the data the only residuals are above  $\sim 25$  keV



The inclusion of relxill model (Garcia & Dauser +14) allows us to measure a cutoff energy  $E_c = 108 \pm 10$  keV and to infer the contribution of the disk to the Compton hump.

# Swift J2127.4+5654



Using compTT (Titarchuk+94) with two different geometries we get:

SLAB

$$kT_e = 68^{+37}_{-32} \text{ keV}$$

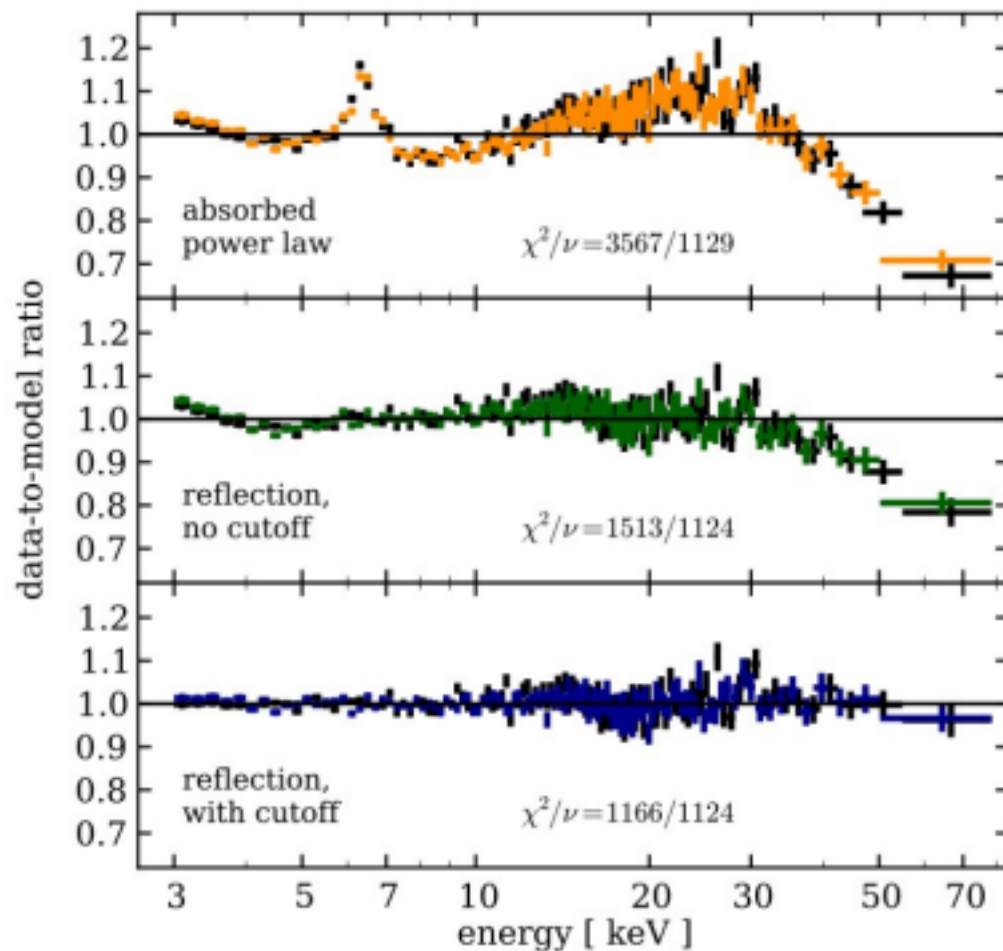
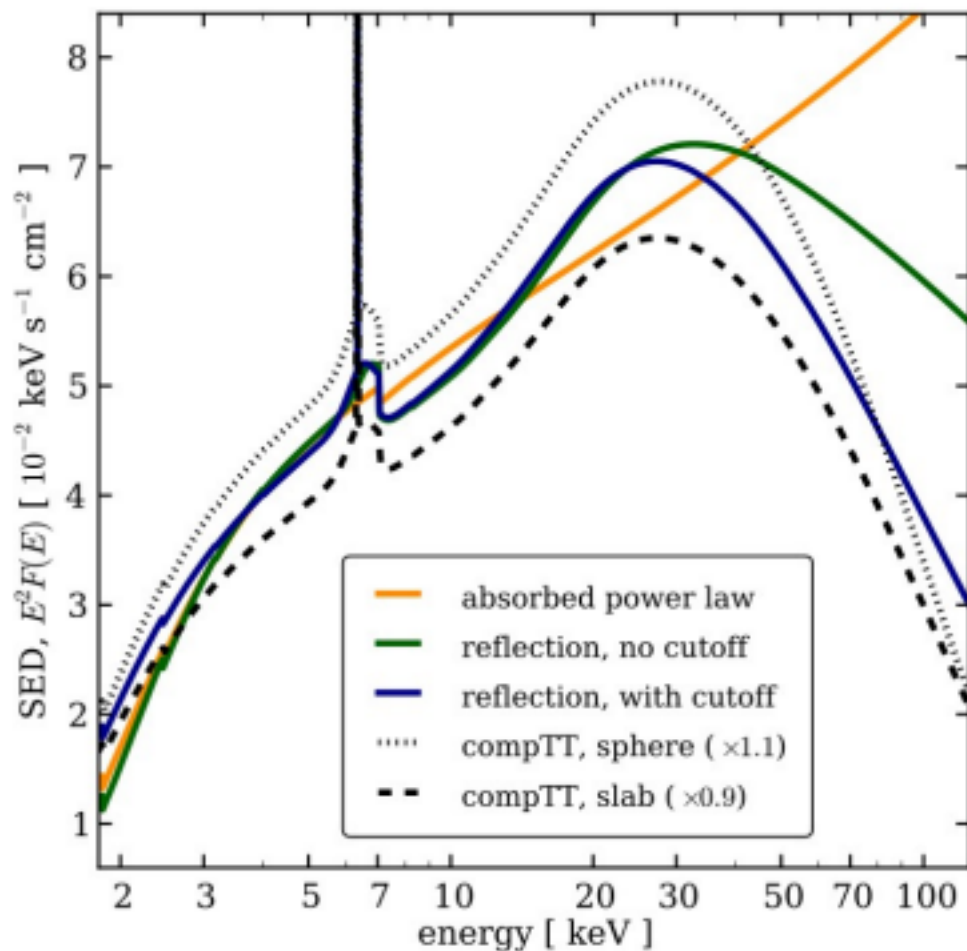
$$\tau = 0.35^{+0.35}_{-0.19}$$

SPHERE

$$kT_e = 53^{+28}_{-26} \text{ keV}$$

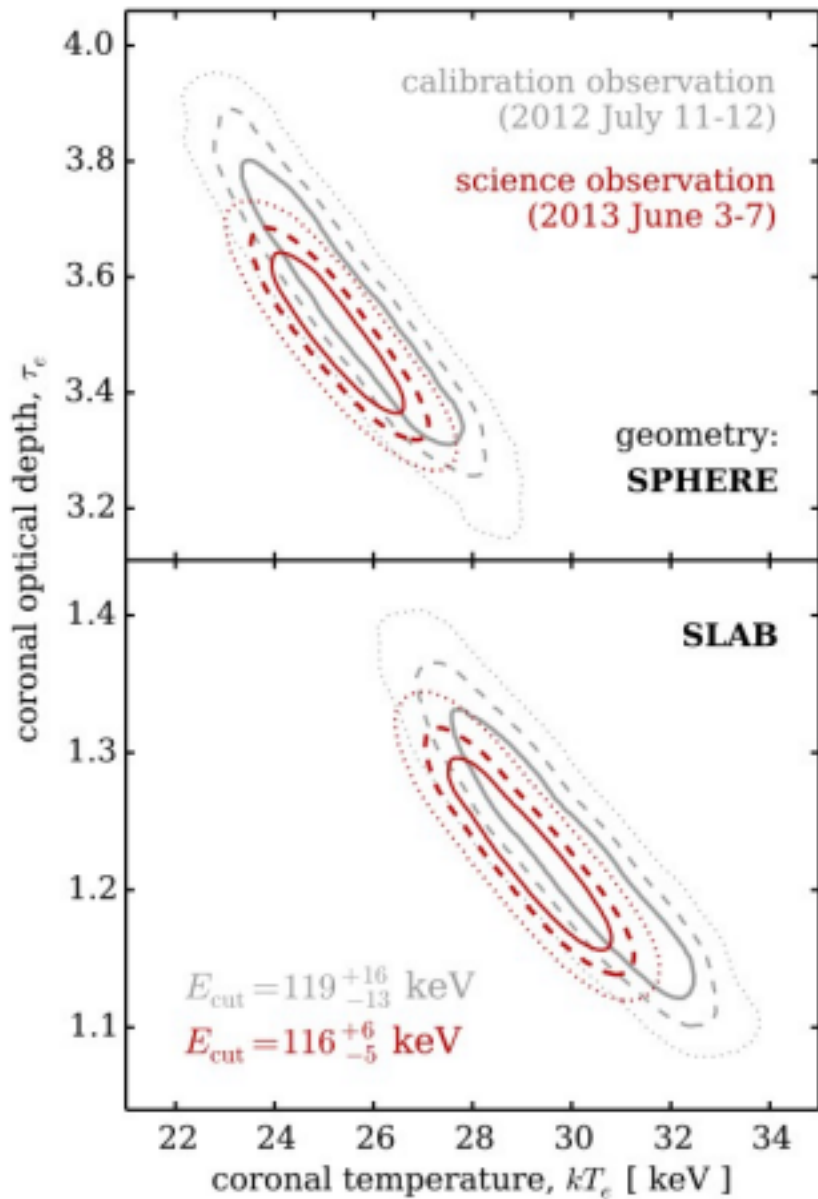
$$\tau = 1.35^{+1.03}_{-0.67}$$

# MCG-05-23-16



Balokovic+15

# MCG-05-23-16

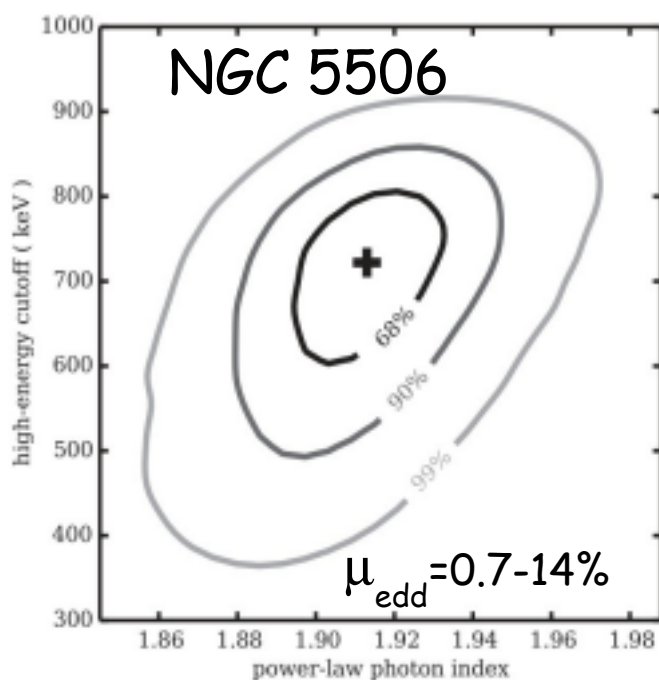


Balokovic+15

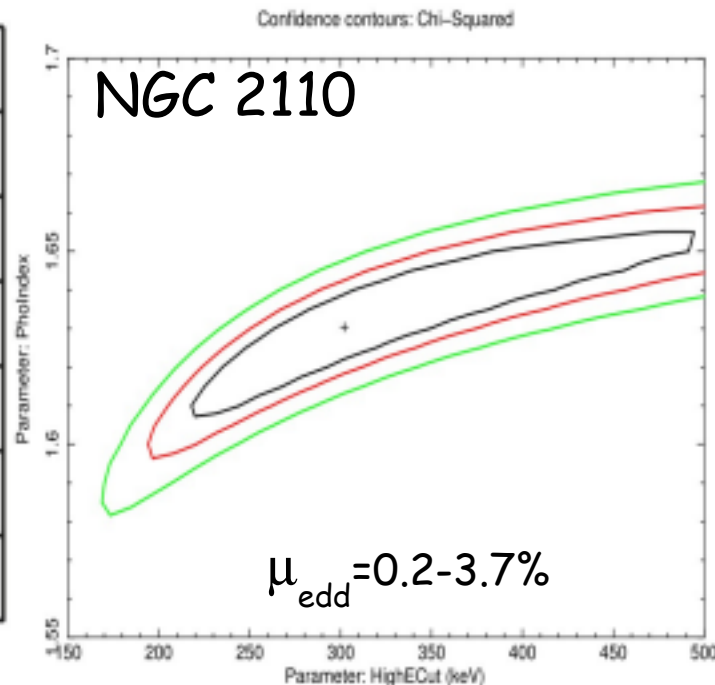
independent of the continuum model		
$C_{\text{FPMB}}^c$	$1.032 \pm 0.002$	$1.045 \pm 0.005$
$E_{\text{line1}}$ [ keV ]	$6.43 \pm 0.05$	$6.5^{+0.2}_{-0.1}$
$\sigma_{\text{line1}}$ [ keV ]	$0.46 \pm 0.06$	$0.5 \pm 0.2$
$\text{EW}_{\text{line1}}$ [ eV ]	$80 \pm 10$	$80 \pm 20$
$\text{EW}_{\text{line2}}$ [ eV ]	$40 \pm 10$	$50 \pm 20$
phenomenological continuum model: pexrav		
$\chi^2$	1163	687
$\Gamma$	$1.85 \pm 0.01$	$1.83 \pm 0.02$
$R$	$0.87 \pm 0.04$	$1.1 \pm 0.1$
$E_{\text{cut}}$ [ keV ]	$116^{+6}_{-5}$	$119^{+16}_{-13}$
Comptonized continuum model: refl(compTT)		
assumed corona geometry: slab		
$\chi^2$	1163	688
$R$	$0.84 \pm 0.04$	$1.1 \pm 0.1$
$kT_e$ [ keV ]	$29 \pm 2$	$30 \pm 3$
$\tau_e$	$1.23 \pm 0.08$	$1.2 \pm 0.1$
assumed corona geometry: sphere		
$\chi^2$	1161	688
$R$	$0.82 \pm 0.04$	$1.0 \pm 0.1$
$kT_e$ [ keV ]	$25 \pm 2$	$26 \pm 3$
$\tau_e$	$3.5 \pm 0.2$	$3.5 \pm 0.3$

# High values/lower limits

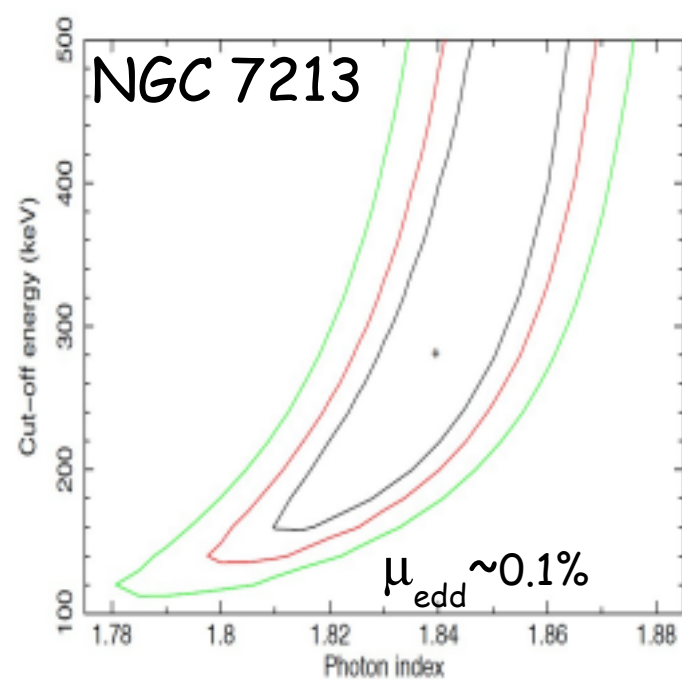
In other bright sources, high values or lower limits to the cutoff energy have been found, suggesting the presence of a very hot corona surrounding the accretion disc.



Matt+15



Marinucci+15

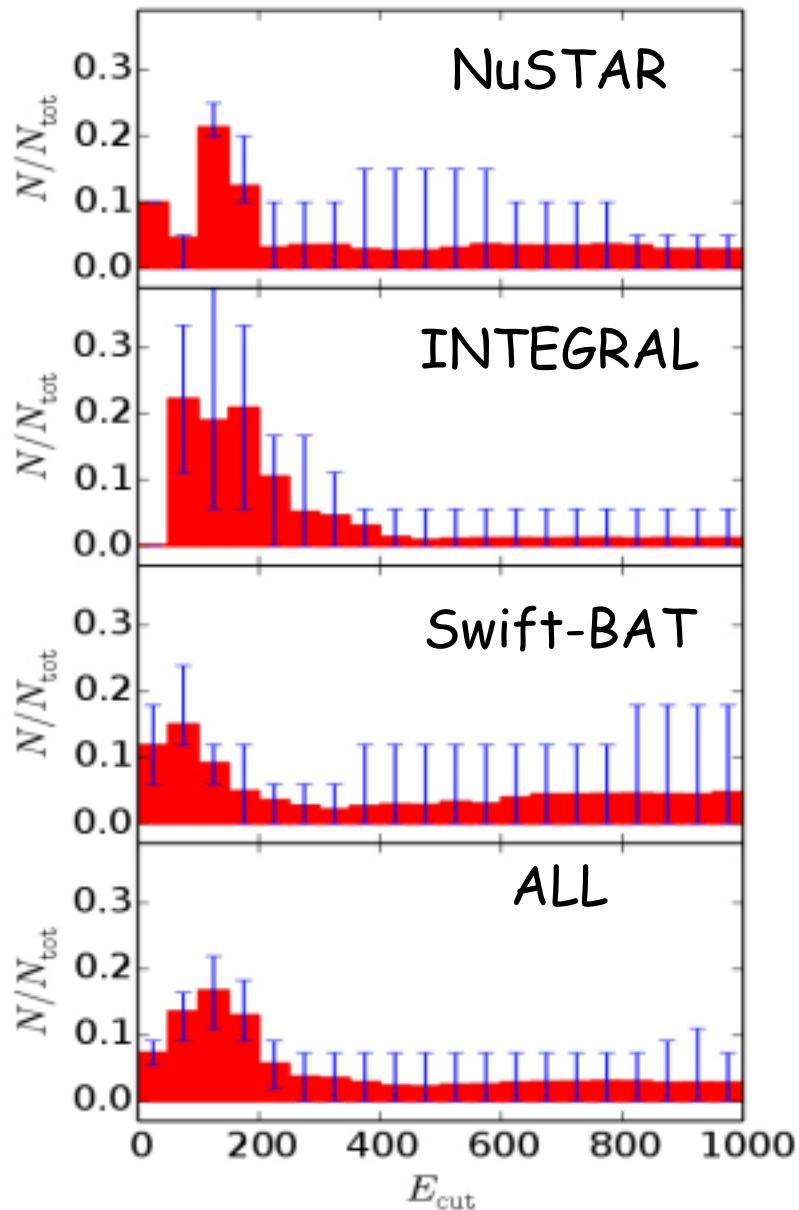


Ursini+15

The next step is to build a small catalog and to start looking for correlations between the coronal temperature and other physical properties (e.g. black hole mass, accretion rate).

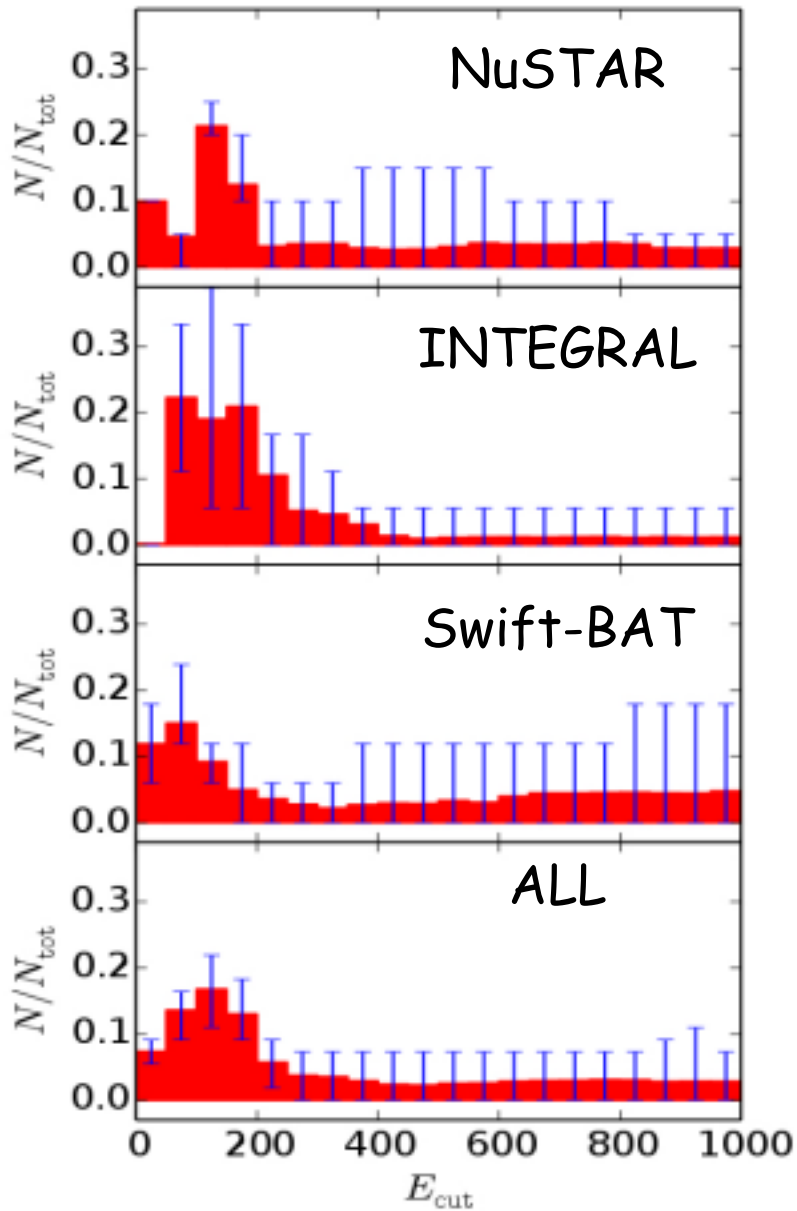


# A larger view

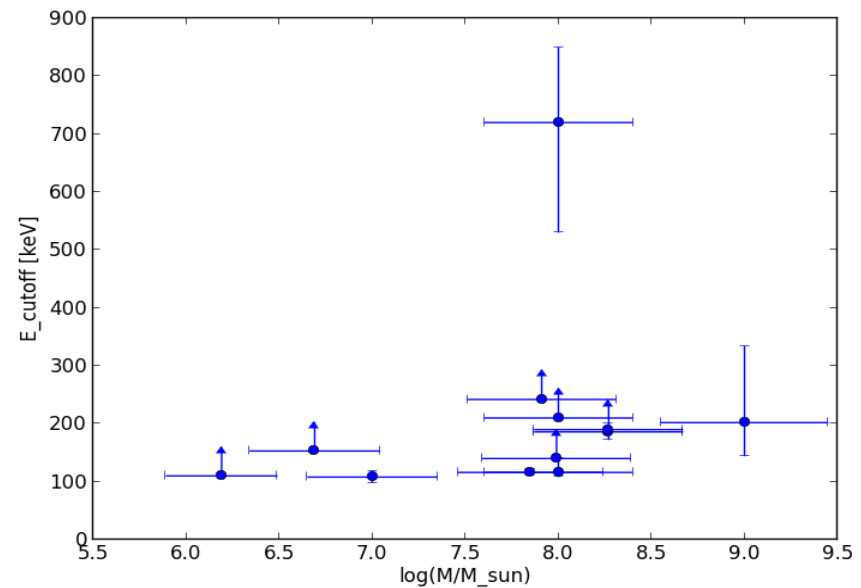
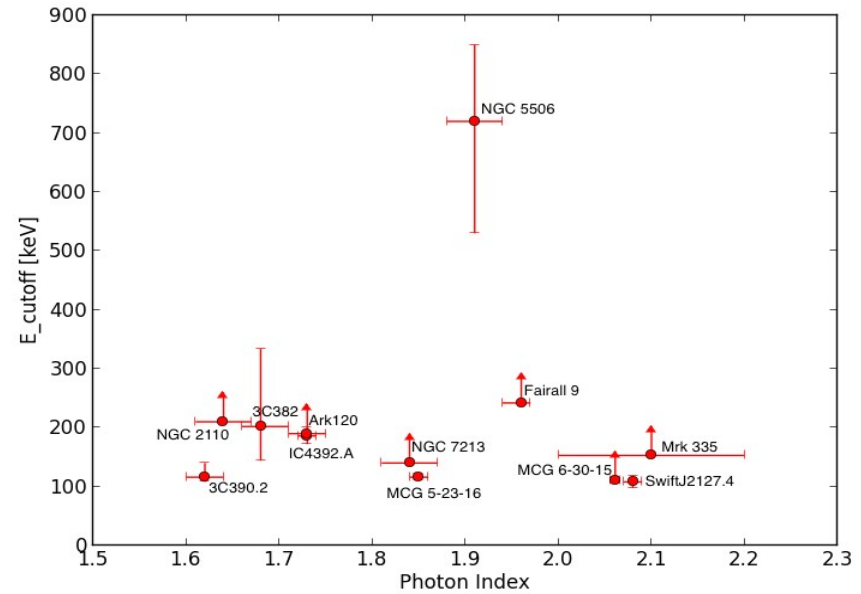


Fabian+15

# A larger view



Fabian+15



Tortosa et al., in prep.



- Brief introduction on high-energy cutoff measurements
  - Nearby AGN seen by NuSTAR
    - Results
- Conclusions and future perspectives

# Conclusions

- High energy cut-off have been measured in a number of AGN with NuSTAR (more are yet to come!)
  - They are not ubiquitous
- The hard X-ray band (3-80 keV) is fundamental for testing and discriminating between different Comptonization models
- Further observations will help us in understanding the nature of the primary continuum, such as the relation between the accretion rate and the cutoff energy and the link between the disc reflection and the extension of the hot corona.